Physiol. Res. 45: 11–22, 1996

Changes of Extracellular Space Volume and Tortuosity in the Spinal Cord of Lewis Rats With Experimental Autoimmune Encephalomyelitis

Z. ŠIMONOVÁ[1], J. SVOBODA[1,2], P. ORKAND[3], C.C.A. BERNARD[4], H. LASSMANN[5], E. SYKOVÁ[1]

[1]Department of Cellular Neurophysiology, Institute of Experimental Medicine, Academy of Sciences of the Czech Republic, Prague, [2]Institute of Physiology and Clinical Physiology, 3rd Medical Faculty, Charles University, Prague, Czech Republic, [3]Institute of Neurobiology, University of Puerto Rico, Old San Juan, U.S.A., [4]Neuroimmunology Laboratory, La Trobe University, Victoria, Australia, [5]Research Unit for Experimental Neuropathology, Austrian Academy of Sciences, Vienna, Austria

Received June 23, 1995
Accepted October 24, 1995

Summary

Three diffusion parameters of nervous tissue, extracellular space (ECS) volume fraction (α), tortuosity (λ) and non-specific uptake (k') of tetramethylammonium (TMA^+), were studied in the spinal cord of rats during experimental autoimmune encephalomyelitis (EAE). The three parameters were determined *in vivo* from concentration-time profiles of TMA^+ using ion-selective microelectrodes. EAE was induced by injection of guinea-pig myelin basic protein (MBP), which resulted in typical morphological changes in the CNS tissue, namely inflammatory reaction, astrogliosis, blood-brain barrier (BBB) damage and paralysis. EAE was accompanied by a statistically significant increase of α (mean±S.E.M.) in the dorsal horn from 0.21±0.01 to 0.28±0.02, in the intermediate region from 0.22±0.01 to 0.33±0.02, in the ventral horn from 0.23±0.01 to 0.47±0.02 and in white matter from 0.18±0.03 to 0.30±0.03. There were significant decreases in tortuosity in the dorsal horn and in the intermediate region and decreases in non-specific uptake in the intermediate region and in the ventral horn. Although the inflammatory reaction and the astrogliosis preceded and greatly outlasted the neurological symptoms, the BBB damage had a similar time course. Moreover, there was a close correlation between the changes in extracellular space diffusion parameters and the manifestation of neurological signs. We suggest that the expansion of the extracellular space alters the diffusion properties in the spinal cord. This may affect synaptic as well as non-synaptic transmission, intercellular communication and recovery from acute EAE, and may contribute to the manifestation of neurological signs in EAE rats.

Key words

Astrogliosis – Diffusion analysis – Oedema – Experimental autoimmune encephalomyelitis – Ion-selective microelectrodes

Introduction

Experimental autoimmune encephalomyelitis (EAE) is widely used as an animal model for the human inflammatory demyelinating disease, multiple sclerosis (MS). EAE as well as MS are characterized by perivascular infiltration, oedema, breakdown of the blood-brain barrier, reactive astrogliosis and demyelination (Lassmann 1983). The clinical signs in rodents with acute EAE observed at the height of the disease reflect particularly intense inflammation, perivascular leukocyte infiltration and vasogenic oedema but little or no demyelination (Lassmann *et al.* 1986, Levine *et al.* 1966). Several studies have shown that the clinical signs are more closely correlated with the extent of oedema in the spinal cord than with the histological evidence of inflammation (Kerlero de Rosbo *et al.* 1985, Leibowitz and Kennedy 1972),

reactive gliosis (Aquino *et al.* 1988, Smith *et al.* 1984) or the degree of demyelination (Lassmann 1983, Raine 1984, Tabira 1988). It has therefore been postulated that the typical clinical signs characterized by a limp tail and hind limb paralysis could be causally related to the occurrence of BBB damage and oedema in the lower spinal cord (Juhler *et al.* 1984, Simmons *et al.* 1982, Wekerle *et al.* 1986). *In vivo* dynamic magnetic resonance imaging (MRI) of EAE rats revealed a correlation between clinical signs and water and protein accumulation in the brain (Namer *et al.* 1992, Seeldrayers *et al.* 1993).

The diffusion properties of the brain and spinal cord have never been examined in EAE rats. Since vasogenic oedema is accompanied by accumulation of extracellular fluid (Klatzo 1987), the extracellular space volume and geometry might be substantially altered. The changes in extracellular space diffusion parameters in the spinal cord of EAE rats could affect diffusion in the extracellular space (ECS) of neuroactive substances, including ions, neurotransmitters, neuropeptides, growth factors, metabolites and drugs used for therapy (Bach-y-Rita 1993, Nicholson 1979, Nicholson and Rice 1991, Syková 1991, 1992), and could also affect cell migration, cell proliferation and remyelination.

Diffusion in ECS obeys Fick's law, subject to two important modifications (Nicholson and Phillips 1981). First, diffusion in ECS is constrained by the restricted volume of the tissue available for diffusing particles, i.e. by the extracellular volume fraction (α). The given quantity of a released substance is therefore more concentrated than it would have been in a free medium. Second, the diffusion coefficient, D, is reduced by the square of the tortuosity (λ) to an apparent diffusion coefficient ADC = D/λ^2, because the diffusing substance encounters membrane obstructions, glycoproteins and macromolecules of the extracellular matrix, and therefore represents the increased path length for diffusion between two points. Besides these two geometrical constraints, the diffusion between cells is affected by non-specific uptake k', the factor describing the loss of material across the cell membranes (Nicholson 1992, Nicholson and Phillips 1981). All three diffusion parameters of the ECS and their dynamic changes can be studied *in vivo* by the real-time iontophoretic method (Nicholson and Phillips 1981), which uses ion-selective microelectrodes to follow the diffusion of an extracellular marker applied by iontophoresis (e.g. the tetramethylammonium ion, TMA^+).

Diffusion parameters in dorsal horns of the spinal cord studied in normal Wistar rats were $\alpha = 0.20 \pm 0.02$, $\lambda = 1.62 \pm 0.01$ and k' = $4.6 \pm 2.5 \times 10^{-3}$ s^{-1} (Syková *et al.* 1994). Changes in spinal cord ECS diffusion parameters (ECS volume decreases and tortuosity increases) have been found to result from activity related to transmembrane ionic shifts and cell swelling during increasing neuronal activity and under pathological conditions such as peripheral injury or ischaemia (Svoboda and Syková 1991, Syková *et al.* 1994). In the present study, diffusion parameters of the ECS were studied in the spinal cord of Lewis rats with EAE. The TMA^+ diffusion profiles were analyzed in control medium (agar), in the grey matter of the dorsal horn, in the intermediate region, in the ventral horn and in the white matter (WM). The three diffusion parameters α, λ (apparent diffusion coefficient) and k' were studied from 7 to 160 days after injection of MBP (dpi) and compared with the clinical score.

Methods

Experimental autoimmune encephalomyelitis (EAE)

Adult Lewis rats (of both sexes) were used in experiments. On day 0, EAE-group rats received an injection of 100 μg of guinea-pig MBP (0.1 ml) emulsified in Complete Freund's Adjuvant (CFA) supplemented with *Mycobacterium tuberculosis* (MT) into both hind foot pads, as previously described (Simmons *et al.* 1981). CFA controls received similar injections except that MBP was omitted from the inoculum. Rats were examined daily throughout the course of the disease and assessed according to the following clinical score: 0: no clinical signs, 1: flaccid tail, 2: mild paraparesis, 3: complete paraplegia accompanied by urinary and faecal incontinence. Histological and electrophysiological studies were performed on control naive rats, control rats which received the injection of CFA and MT, and in the following groups of EAE rats: 7–10 dpi (clinical score 0), 14–17 dpi (clinical score 2–3), 20–22 dpi (clinical score 0–1) and 40–60 dpi, 105 dpi, 160 dpi (clinical score 0) (see Fig. 3).

For electrophysiological recordings, the rats were anaesthetised with pentobarbital (40–60 mg/kg i.p.) and were given further injections of the anaesthetic during the experiments (10–20 mg/kg approximately each hour). A laminectomy was performed between L2 and L6. The animals were artificially ventilated and immobilized with an intramuscular injection of D-tubocurarine. The body temperature, arterial blood pressure and heart rate were monitored. The animals were mounted in a rigid frame, and a pool filled with paraffin oil (37 °C) was made around the spinal cord by fixing the skin flaps to a frame. To minimize respiratory movements at the lumbar level, the chest was suspended free of the underlying surface, using the spinous processes for attachment.

Histological and immunohistochemical studies

Randomly selected rats were sacrificed after electrophysiological recordings for histological and

immunohistochemical studies (n=10), but sometimes additional animals were used (n=22). Animals were perfused transcardially with saline followed by a mixture of 4 % paraformaldehyde in 0.1 M phosphate buffered saline (PBS, pH 7.5). The spinal cord was dissected and after 4 hours of fixation immersed in PBS with 30 % saccharose, and cut on a cryostat. Staining of cell nuclei with Nuclear Fast Red (Sigma) was used to follow inflammatory reactions. The BBB leakage was identified using specific antibodies: rabbit anti-rat albumin or rabbit anti-rat immunoglobulin (IgG). Astrogliosis was studied using rabbit antibodies to glial fibrillary acidic protein (GFAP, Sigma). After the primary antibody, the Vectastain Elite ABC kit (Vector Laboratories) with biotinylated secondary antibodies followed by avidin and biotinylated horseradish peroxidase macromolecular complex was used. Immune complexes were visualized by 3,3'-diaminobenzidine tetrachloride (DAB, Sigma) and H_2O_2. The sections (12 μm thick) were covered by an acrylic mounting medium (Solacryl, Sanitas, CR).

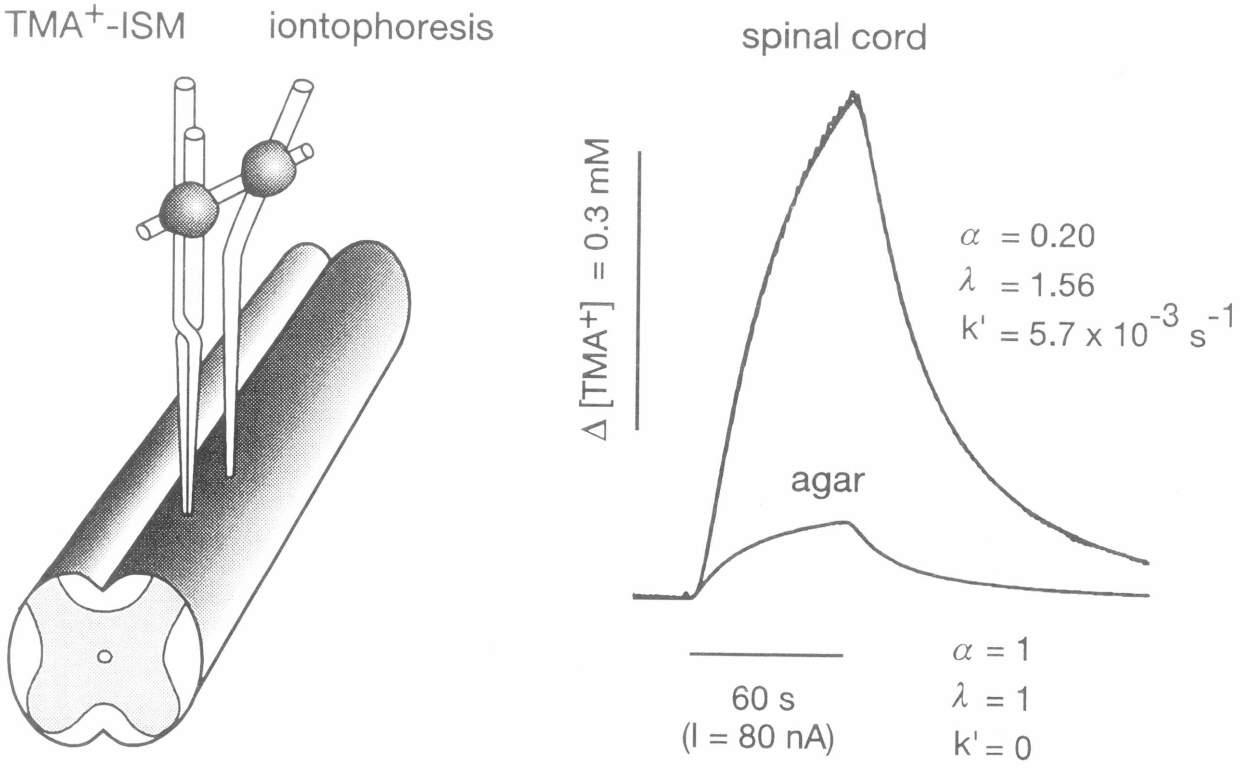

Fig. 1

Experimental procedure. Left: Scheme of the experimental arrangement. TMA$^+$-selective double-barrelled ion-selective microelectrode (ISM) was glued to a bent iontophoresis microelectrode. The separation between electrode tips was 100–200 µm. Right: Typical records obtained with this set-up in the spinal cord of a Lewis rat. In this Figure, as well as in Fig. 4, the concentration scale is linear and the theoretical diffusion curve (Equation 1) is superimposed on each data curve. When the electrode array was inserted into the spinal dorsal horn and the iontophoretic main current applied, the resulting increase in concentration was much larger in the spinal cord than that in agar gel, apparently due to a larger volume fraction. The separation between the ISM and iontophoresis electrode tips was 200 µm. The values of α, λ and k' are shown with each record. Both recordings were made in the same animal with one microelectrode array. Electrode transport number n = 0.477.

Measurements of ECS diffusion parameters

Ion-selective microelectrodes (ISMs) were used to measure TMA^+ diffusion parameters in ECS. Double-barrelled ISMs for TMA^+ were made as described elsewhere (Syková *et al.* 1994). The ion exchanger was a Corning 477317 and the ion-sensing barrel was back-filled with 100 mM TMA chloride, while the reference barrel contained 150 mM NaCl. The electrodes were calibrated using the fixed-interference method before and after each experiment in a sequence of solutions of 150 mM NaCl + 3 mM KCl with the addition of the following amounts of TMA chloride (mM): 0.0003, 0.001, 0.003, 0.01, 0.03,

0.1, 0.3, 1.0, 3.0, 10.0. The calibration data were fitted to the Nikolsky equation to determine the electrode slope and interference.

For TMA^+ diffusion measurements, iontophoresis pipettes were prepared from theta glass. The shank was bent before back-filling with 1 M TMA chloride, so that it could be aligned parallel to that of the ISM. Electrode arrays were made by gluing together an iontophoresis pipette and a TMA^+-ISM with a tip separation of 130–200 μm (Fig. 1). Typical iontophoresis parameters were +20 nA bias current (continuously applied to maintain a constant transport number) and +80 nA current step with 60 s duration to generate the diffusion curve. TMA^+ diffusion curves were captured on a digital oscilloscope (Nicolet 3091), then transferred to a PC-compatible, 486 computer where they were analyzed by fitting the data to a solution of the diffusion equation (1) using the program VOLTORO (Nicholson, unpublished).

The TMA^+ concentration vs. time curves were first recorded in 0.3 % agar gel (Difco, Special Noble Agar) made up in 150 mM NaCl, 3 mM KCl and 0.3 mM TMA^+ in a Lucite cup that could be placed just above the spinal cord. The array of electrodes was then lowered into the spinal cord to appropriate depths. The diffusion curves obtained were analyzed to yield α and λ and the non-specific, concentration-dependent uptake term, k' (s^{-1}). These three parameters were extracted by a non-linear curve-fitting simplex algorithm operating on the diffusion curve described by Equation (1) below, which represents the behaviour of TMA^+, assuming that it spreads out with spherical symmetry, when the iontophoresis current is applied for duration S. In this expression, C is the concentration of the ion at time t and distance r. The equation governing the diffusion in brain tissue is:

$$C = G(t) \qquad t < S,$$

for the rising phase of the curve.

$$C = G(t)-G(t-S) \qquad t > S,$$

for the falling phase of the curve.

The function G(u) is evaluated by substituting t or t−S for u in the following equation (Nicholson 1992):

$$G(u) = (Q\lambda^2/8\pi D)\alpha r)\{\exp[r)\lambda(k'/D)^{1/2}]$$
$$\operatorname{erfc}[r\lambda/2(Du)^{1/2} + (k'u)^{1/2}] + \exp[-r\lambda(k'/D)^{1/2}]$$
$$\operatorname{erfc}[r\lambda/2(Du)^{1/2} - (k-u)^{1/2}]\} \qquad (1)$$

The quantity of TMA^+ delivered to the tissue per second is Q = In/zF, where I is the step increase in current applied to the iontophoresis electrode, n is the transport number, z is the number of charges associated with substance iontophoresed (+ 1 here) and F is Faraday—s electrochemical equivalent. The function "erfc" is the complementary error function. When the experimental medium is agar, by definition, $\alpha = 1 = \lambda$ and k' = 0 (Fig. 1) and the parameters n and D are extracted by the curve fitting. Knowing n and D, the parameters α, λ and k' can be obtained when the experiment is repeated in the spinal cord (Fig.1).

Results

Histological and immunohistochemical changes in the spinal cord

In control animals, only some lymphocytes were found in the meninges and few in the grey matter. In EAE rats, the inflammatory reaction seen in the CNS consisted of massive perivascular infiltration of the tissue with lymphocytes, monocytes and macrophages. The infiltrates were found around many large as well as small blood vessels, suggesting their leakage (Fig. 2a). Inflammatory reactions did not precede clinical manifestation of EAE and were most prominent 17–24 days after the injection of MBP; i.e. it clearly outlasted the period of maximal neurological signs at 15–18 dpi (Fig. 3 A,B). No inflammatory reaction was found at 56, 105 and 160 dpi.

In control animals, immunostaining with anti-GFAP revealed typically mature types of astrocytes. Immunoreactivity for GFAP was found in fine star-shaped processes. Some GFAP-stained astrocytes were attached to the blood vessels. In EAE animals, immunoreactivity for GFAP had already increased at 12 dpi and peaked at 14-15 dpi, but it persisted at 24, 56, 105 and 160 dpi (Fig. 2b), exhibiting thicker and longer processes that often impinged upon the walls of blood vessels and capillaries (Fig. 2b; see also D'Amelio *et al.* 1990). It is therefore evident that astrocytic proliferation and hypertrophy outlasted neurological signs of EAE by many days (Fig. 3 C).

Fig. 2c further shows the albumin leakage due to the BBB breakdown, suggesting oedema formation in the spinal cord. The light and diffuse albumin or IgG leakage was found at 9 dpi; however, dramatic leakage with massive leakage around blood vessels was observed between 15-18 dpi (Fig. 3 D). Light diffuse staining was apparent at 24 dpi, while no signs of BBB damage were seen at 56, 105 and 160 dpi. The time course of BBB damage therefore only slightly preceded and outlasted the neurological signs in EAE rats (Fig. 3 A).

Fig. 2

Inflammation, astrogliosis and BBB leakage in the spinal cord of EAE rats. a: Infiltration of the spinal cord by lymphocytes occurring around the blood vessels. Staining of lymphocyte nuclei with Nuclear Fast Red, section from an animal 24 dpi, b: Astrogliosis revealed by anti-GFAP staining in an animal 15 dpi. Note densely stained reactive astrocytes. c: BBB damage revealed by albumin leakage. Anti-albumin staining in an animal at 15 dpi. Scale bars: a = 100 μm, b = 20 μm, c = 50 μm.

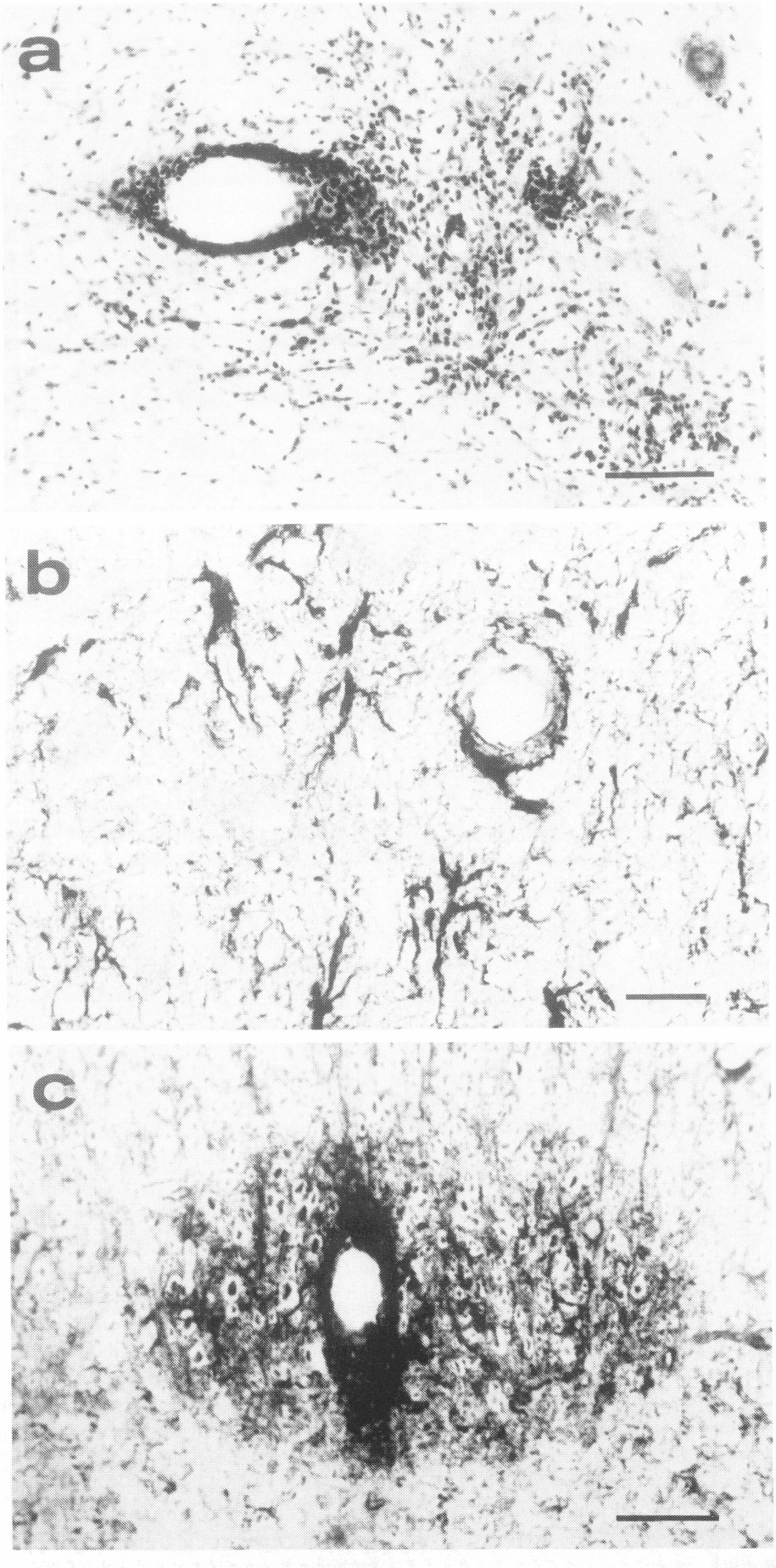
a
b
c

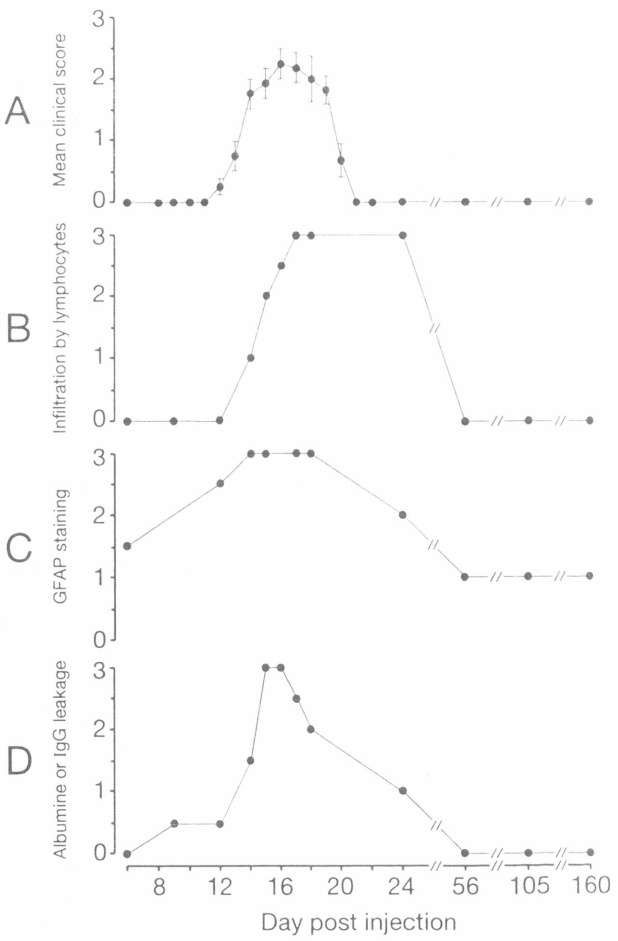

Fig. 3

Time course of inflammation, astrogliosis, BBB damage, neurological signs (clinical score) and changes in extracellular space diffusion parameters in the spinal cord of EAE rats. A – Clinical score: 0: no signs, 1: flaccid tail, 2: mild paraparesis, 3: severe paraparesis with incontinence (mean ± S.E.M. , n=24). B – Inflammation: 1: number of lymphocyte nuclei stained increased particularly around blood vessels; 2: diffuse staining in whole spinal cord with more nuclei stained around blood vessels, staining more intensive than in 1; 3: large clusters of nuclei around blood vessels full of lymphocytes, more intensive staining than in 2. C – Astrogliosis: 1: in comparison with control animal, GFAP staining revealed spots in grey matter with short, thicker and more densely stained processes; 2: processes become thicker and more densely stained throughout the whole spinal cord, including white matter; 3: an overall density of GFAP staining increased, thick processes were present in grey and white matter. D – BBB damage: 1: Light diffuse staining in grey matter; 2: diffuse staining was accompanied by more densely stained areas around blood vessels; 3: dense and diffuse staining of the grey matter with larger and more densely stained areas around blood vessels. B – D: Each point is mean value from two animals, when at least 10 sections were inspected in each animal.

Diffusion parameters in grey and white matter

The extracellular space volume fraction α, tortuosity λ and the non-specific uptake k' have been studied in the spinal dorsal horn of Wistar rats previously (Svoboda and Syková 1991, Syková *et al.* 1994). These papers revealed that afferent stimulation or the acute phase of peripheral injury (formalin or turpentine injection into the hind paw) resulted in decreases of α, with no significant changes in λ and k'. However, the changes after the formalin or turpentine injection did not last more than two hours. We found no significant difference in spinal cord diffusion parameters in naive Wistar rats (Syková *et al.* 1994), in naive Lewis rats (n=17) or in Lewis rats which received CFA and MT and were tested 7–24 dpi (n=10). Figure 1 shows an example of the TMA^+ diffusion curve in agar as compared with the diffusion curve recorded with the same microelectrode array in the spinal intermediate region of a control (naive) Lewis rat.

The diffusion parameters and field potentials in EAE rats were studied in the seven groups according to the clinical score, namely at 7 and 10 dpi (before any neuropathological manifestation), at 14 and 17 dpi (during maximal clinical signs), at 20 and 22 dpi (during recovery, when only weak paresis persisted) and at 40–60 dpi, when no neuropathological signs could be detected. Table 1 summarizes the results of the diffusion studies (mean ± S.E.M.) in four areas of the spinal cord, namely in the dorsal horn (at depth 250–500 μm from the dorsal surface), in the intermediate region (at a depth 750–1250 μm), in the ventral horn (at a depth 1500–2250 μm) and in the white matter (at a depth 2500–3000 μm). The localization of the microelectrodes in these areas was confirmed by some experiments (n=11) in which measurements were taken after the spinal cord has been removed, cooled in saline and sliced with a razor blade or by a vibrocat (WPI). No statistically different values of α, λ and k' were found in the spinal cord of naive rats or EAE rats at 7–10 dpi, although the values were generally higher in the EAE rats. However, in EAE rats during the period of maximal clinical signs, i.e. at 14–17 dpi, the extracellular space volume fraction (α) increased significantly in the dorsal horn, in the intermediate region, in the ventral horn, and in the white matter. Concomitantly with the increase in α, λ significantly decreased in the dorsal horn and in the intermediate region, while k' decreased in the intermediate region and in the ventral horn (Table 1).

Fig. 4a shows normal diffusion parameters at various spinal cord depths of a control Lewis rat. In this experiment, the values of α varied typically between 0.18–0.24 and λ between 1.5–1.65. There was the typical field potential evoked by a single electrical pulse of supramaximal intensity, applied to the sciatic nerve and recorded at a depth of 750 μm.

Table 1

ECS diffusion parameters in control and EAE rats at various depths of the spinal cord as measured from the dorsal surface as a function of days after the injection of MBP (EAE dpi) and the clinical score (0–3). α is ECS volume fraction, λ is ECS tortuosity, k' is non-specific cellular uptake, n is the number of animals. From 3 to 10 diffusion curves were recorded in each area of an animal to ensure stable values. Statistical analysis of the differences between control and experimental animals was evaluated using the one–way ANOVA test. *** $p<0.001$, ** $p<0.01$, * $p<0.05$.

EAE dpi (score)	n	250 - 500 μm	750 - 1250 μm	1500 - 2250 μm	2500 - 3000 μm
Control	27	α = 0.21 ± 0.014 λ = 1.55 ± 0.045 k' = 8.2 ± 1.5 x 10^{-3} s^{-1}	α = 0.22 ± 0.006 λ = 1.54 ± 0.025 k' = 6.7 ± 0.9 x 10^{-3} s^{-1}	α = 0.23 ± 0.007 λ = 1.46 ± 0.016 k' = 5.7 ± 1.2 x 10^{-3} s^{-1}	α = 0.18 ± 0.029 λ = 1.56 ± 0.041 k' = 8.3 ± 3.6 x 10^{-3} s^{-1}
7 - 10 (0)	5	α = 0.25 ± 0.012 λ = 1.47 ± 0.030 k' = 8.1 ± 2.7 x 10^{-3} s^{-1}	α = 0.24 ± 0.032 λ = 1.57 ± 0.080 k' = 2.9 ± 0.5 x 10^{-3} s^{-1}	α = 0.22 ± 0.038 λ = 1.47 ± 0.094 k' = 10.9 ± 3.8 x 10^{-3} s^{-1}	α = 0.24 ± 0.020 λ = 1.53 ± 0.097 k' = 4.3 ± 0.1 x 10^{-3} s^{-1}
14 - 17 (2 - 3)	13	α = 0.28 ± 0.021 ** λ = 1.40 ± 0.043 * k' = 2.9 ± 2.2 x 10^{-3} s^{-1}	α = 0.33 ± 0.024 *** λ = 1.42 ± 0.036 ** k' = 2.0 ± 0.6 x 10^{-3} s^{-1} **	α = 0.47 ± 0.020 *** λ = 1.48 ± 0.062 k' = 3.0 ± 0.4 x 10^{-3} s^{-1} **	α = 0.30 ± 0.030 ** λ = 1.48 ± 0.076 k' = 1.1 ± 0.2 x 10^{-3} s^{-1}
20 - 22 (0 - 1)	6	α = 0.25 ± 0.025 λ = 1.54 ± 0.077 k' = 3.8 ± 2.0 x 10^{-3} s^{-1}	α = 0.31 ± 0.033 *** λ = 1.50 ± 0.054 k' = 3.7 ± 0.7 x 10^{-3} s^{-1}	α = 0.28 ± 0.037 * λ = 1.51 ± 0.054 k' = 2.7 ± 0.3 x 10^{-3} s^{-1} *	α = 0.20 ± 0.045 λ = 1.40 ± 0.034 k' = 3.0 ± 0.4 x 10^{-3} s^{-1}
40 - 60 (0)	11	α = 0.21 ± 0.016 λ = 1.49 ± 0.068 k' = 4.8 ± 0.5 x 10^{-3} s^{-1}	α = 0.24 ± 0.013 λ = 1.59 ± 0.056 k' = 5.5 ± 0.4 x 10^{-3} s^{-1}	α = 0.26 ± 0.023 λ = 1.50 ± 0.076 k' = 7.9 ± 1.0 x 10^{-3} s^{-1}	α = 0.20 ± 0.018 λ = 1.46 ± 0.065 k' = 10.7 ± 5.0 x 10^{-3} s^{-1}

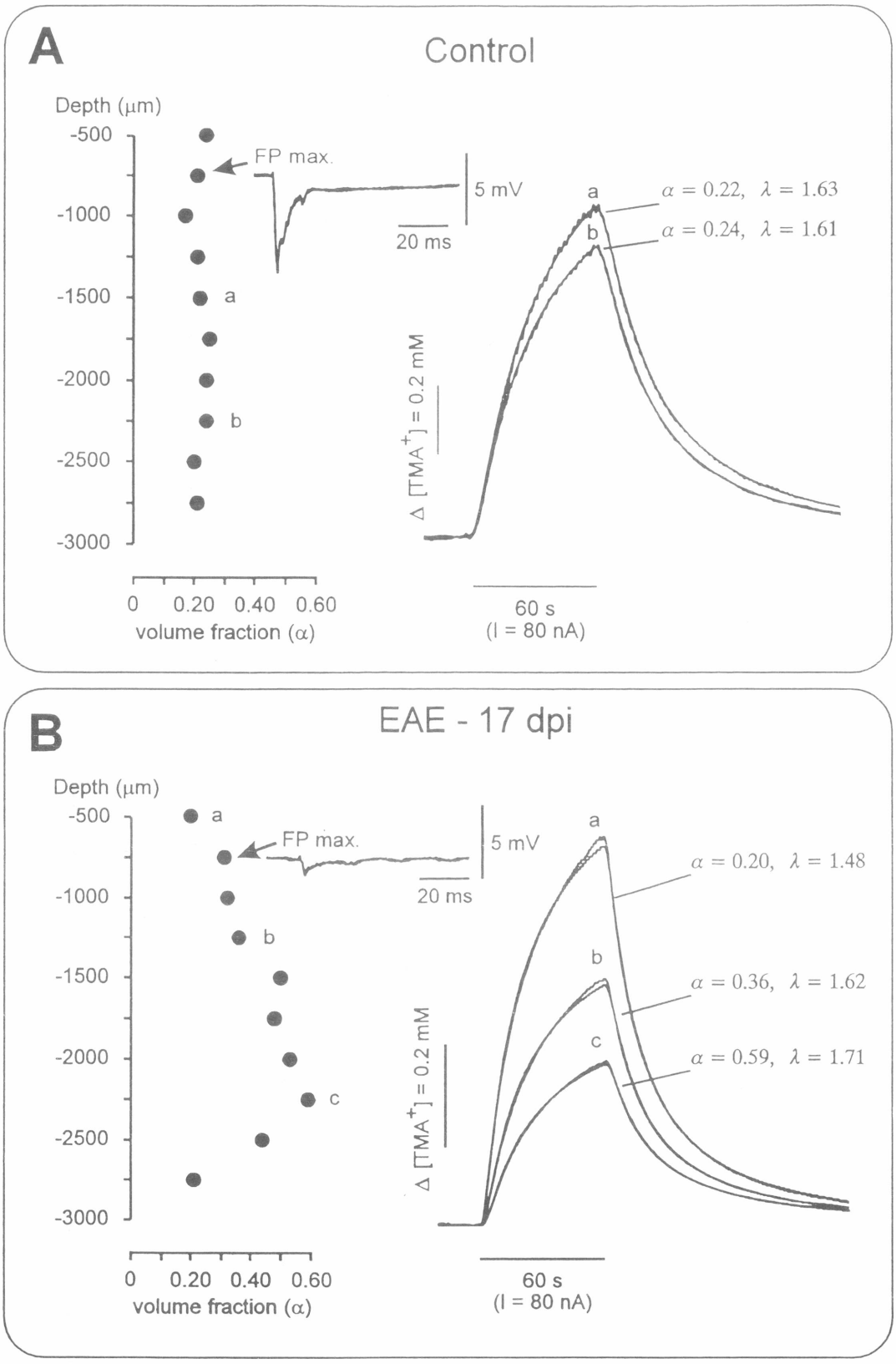

Fig. 4

Extracellular space volume fraction (α) at various depths in spinal cord segment L4 of a control (A) and EAE (B) Lewis rat as measured from the dorsal surface. Representative diffusion curves are shown on the right together with values of α and λ. FP max. : Largest field potentials recorded in dorsal horn with reference barrel of ion-selective microelectrode was recorded at a depth 750 μm. A: The array spacing was 180 μm, electrode transport number n = 0. 669. B: The array spacing was 140 μm, electrode transport number n = 0.323.

Fig. 4b shows the values of α at various depths and typical diffusion curves in an EAE rat spinal cord at 17 dpi. In this rat, with a clinical score of 3, maximal changes of α were found in the ventral horn. The field potentials recorded in the dorsal horn (at depth 750 μm) were substantially smaller than those in control rats. In the individual animals with EAE, the maximal changes in α occurred either in the intermediate region or in the ventral horn (Fig. 4b). Our results also show that in some regions in the spinal cord of individual animals with EAE, the ECS volume was more than doubled, while in others there was no significant difference from control rats.

In EAE rats at 20–22 dpi, some of which showed modest neuropathological signs (Fig. 3d), α was still significantly increased in the intermediate region and in the ventral horns, although these values were already lower than those at 14–17 dpi (Table 1). In these rats, k' was still lower in the ventral horns; however, λ was not significantly different from those of the controls. Diffusion parameters in animals at 40–60 dpi were not significantly different from those in control rats (Table 1).

Discussion

Vasogenic oedema and BBB damage have been found to be associated with many neurological diseases, including multiple sclerosis (MS) (for review see Adams 1983 and Lassmann 1983) as well as acute inflammation of the brain (Betz *et al.* 1989, Fishman 1980). Vasogenic oedema is usually accompanied by extracellular accumulation of fluid (Klatzo 1987). Our results unequivocally show that the inflammatory reaction and BBB breakdown in EAE rats result in dramatic and substantial changes in spinal cord extracellular space diffusion parameters, particularly extracellular space volume in both grey and white matter, but also ECS geometry (tortuosity). The time course of the clinical signs corresponded to increases in α, suggesting a possible causal relationship.

Recently, Lo and colleagues (1993) studied the changes in extracellular space diffusion parameters in an experimental model of brain abscess during which brain oedema may develop. In their study, acute inflammation was accompanied by an increase in BBB permeability in the abscess region. However, the inflammation evoked by intracerebral inoculation with a weakly pathogenic strain of *Staphylococcus aureus* was not accompanied by significant changes in the diffusion properties of the cortical extracellular space, although, as the authors state, "volume fraction tended to be somewhat larger and the tortuosity somewhat smaller at 1000 μm from the surface." However, the same authors also found a lack of change in the water content of the inoculated region, indicating that there was no significant development of brain oedema in the cortex.

Assuming that the changes in λ reflect a change in the apparent diffusion coefficient (ADC) of TMA^+, $\lambda = (D/ADC)^{1/2}$, where D is the free diffusion coefficient of TMA^+, then our experiments on EAE rats also show that ADCs of TMA^+ (and apparently also of other compounds of similar low molecular weight) are increasing. Clinical data obtained with nuclear magnetic resonance (NMR) show increases in the ADC of water in patients with multiple sclerosis. In rats with EAE, MRI measurements *in vivo* revealed a close correlation between increases of relaxation times T1 and T2 and the BBB permeability visualized by gadolinium-DTPA intravenous injection (Namer *et al.* 1992, 1993). Furthermore, gadolinium-DTPA leakage correlated well with the time course and degree of CNS inflammation in the early stages of EAE, whereas in the late stages persistent inflammation was present, but BBB damage of gadolinium-DTPA had subsided (Seeldrayers *et al.* 1993). The resulting changes in MR images might be due to changes in the ADC of water in normal and oedematous tissue. However, the NMR technique can in principle detect both intracellular and extracellular water. Our measurements show a close correlation with the changes in ECS diffusion parameters, particularly with the ECS volume increase (Table 1).

Astrocytic swelling frequently occurs in pathological states, including EAE (Yu *et al.* 1992). Although this swelling is accompanied by compensatory ECS shrinkage, no decreases of ECS volume have been found in the spinal cord of EAE rats. Similarly, as was shown by others (Smith *et al.* 1983, Goldmuntz *et al.* 1986, Aquino *et al.* 1988, Eng *et al.* 1989, D'Amelio *et al.* 1990), increases in GFAP staining in the spinal cord of EAE rats preceded and outlasted the clinical signs. In our experiments, GFAP staining was already elevated at 12 dpi, and remained elevated at 160 dpi (Fig. 3 C). This reaction of astrocytes also preceded the time when the bulk of inflammatory cells – macrophages and T-lymphocytes – begin to penetrate the capillary walls (Fig. 3 B, see also D'Amelio *et al.* 1990, Vass *et al.* 1986). The invasion of the tissue by inflammatory cells correlated with the occurrence of clinical signs and with the beginning of the changes in the ECS diffusion parameters, but it outlasted them substantially (Fig. 3 B, see also Lassmann *et al.* 1986, D'Amelio *et al.* 1990).

While some authors argue that neurological signs of acute EAE are due to demyelination in the PNS and CNS (Pender *et al.* 1989), demyelination is not a prominent feature in the early stages of EAE (Kerlero de Rosbo *et al.* 1985, Lassmann *et al.* 1986). Because the time course of demyelination was not followed in this study, we cannot exclude the possibility that some of the increase in ECS volume fraction

observed at 14–17 dpi is the result of demyelination rather than oedema.

There is no question that fluid accumulates in active MS lesions due to BBB damage (McDonald *et al.* 1992). In EAE rats, BBB breakdown and oedema have been described repeatedly. Clinical signs occurring independently of demyelination coincided with vasogenic oedema (Kerlero de Rosbo *et al.* 1985, Namer *et al.* 1993). In our experiments, a close correlation has been found between peak BBB permeability and the manifestation of neurological signs, but modest BBB leakage preceded and outlasted the clinical signs (Fig. 3 D). On the other hand, significant changes in the extracellular space volume fraction in individual animals exactly matched the severity and time course of the neurological signs. This suggests the possibility that the paralysis is partly caused by changes in the diffusion parameters of ions, transmitters, neuromodulators and metabolites in synaptic clefts as well as in the ECS, altering synaptic as well as non-synaptic transmission in the spinal cord and communication between neurones and between neurones and glia.

Acknowledgement

The authors thank Prof. Charles Nicholson for providing us with his VOLTORO program and helpful comments. This work was supported by grant GA CR no. 309/93/1048, grant GA CR no. 309/94/1107, U.S. - Czech Science and Technology Program Award no. 92048, and the National Health and Medical Research Council of Australia (CCAB).

References

ADAMS C. W. M.: The general pathology of multiple sclerosis: morphological and chemical aspects of the lesions. In: *Multiple Sclerosis.* J.F. HALLPIKE, C.W.M. ADAMS, W.W. TOUTELLOTTE (eds), Chapman and Hill, London, 1983, pp. 203–240.

AQUINO D.A., CHIU F.-C., BROSNAN C.F., NORTON W.T.: Glial fibrillary acidic protein increases in the spinal cord of Lewis rats with acute experimental autoimmune encephalomyelitis. *J. Neurochem.* **51:** 1085–1096, 1988.

BACH-Y-RITA P.: Neurotransmission in the brain by diffusion through the extracellular fluid: a review. *Neuroreport* **4:** 343–350, 1993.

BETZ A.L., IANNOTI F., HOFF J.: Brain edema: a classification based on blood-brain barrier integrity. *Cerebrovascular and Brain Metabolism Reviews* **1:** 133–154, 1989.

D'AMELIO F.E., SMITH M.E., ENG L.F.: Sequence of tissue responses in the early stages of experimental allergic encephalomyelitis (EAE): Immunohistochemical, light microscopic, and ultrastructural observations in the spinal cord. *Glia* **3:** 229–240, 1990.

ENG L.F., D'AMELIO F.E., SMITH M.E.: Dissociation of GFAP intermediate filaments in EAE: observations in the lumbar spinal cord. *Glia* **2:** 308–317, 1989.

FISHMAN R.A.: *Cerebrospinal Fluid in Diseases of the Nervous System.* W.B. Saunders, Philadelphia, 1980, pp. 113–121.

GOLDMUNTZ E.A., BROSNAN C.F., CHIU F.-C., NORTON W.T.: Astrocytic reactivity and intermediate filament metabolism in experimental autoimmune encephalomyelitis: the effect of suppression with prazosin. *Brain Res.* **397:** 16–26, 1986.

JUHLER M., BARRY D.I., OFFNER H., KONAT G., KLINKEN L., PAULSON O.B.: Blood-brain and blood-spinal cord barrier permeability during the course of experimental allergic encephalomyelitis in the rat. *Brain Res.* **302:** 347–355, 1984.

KERLERO DE ROSBO N., BERNARD C.C.A., SIMMONS R.D., CARNEGIE P.R.: Concomitant detection of changes in myelin basic protein and permeability of blood/spinal cord barrier in acute experimental autoimmune encephalomyelitis by electroimmunoblotting. *J. Neuroimmunol.* **9:** 349–361, 1985.

KLATZO I.: Pathophysiological aspects of brain edema. *Acta Neuropathol.* **72:** 236–239, 1987.

LASSMANN H.: *Comparative Neuropathology of Chronic Experimental Allergic Encephalomyelitis and Multiple Sclerosis.* Springer, Berlin, 1983.

LASSMANN H., VASS K., BRUNNER CH., SEITELBERGER F.: Characterization of inflammatory infiltrates in experimental allergic encephalomyelitis. *Progr. Neuropathol.* **6:** 33–62, 1986.

LEIBOWITZ S., KENNEDY L.: Cerebral vascular permeability and cellular infiltration in experimental allergic encephalomyelitis. *Neurology* **22:** 859–869, 1972.

LEVINE S., SIMON J., WENK E.J.: Edema of the spinal cord in experimental allergic encephalomyelitis. *Proc. Soc. Exp. Biol. Med.* **123:** 539–541, 1966.

LO W.D., WOLNY A.C., TIMAN C., SHIN D., HINKLE G.H.: Blood-brain barrier permeability and the brain extracellular space in acute cerebral inflammation. *J. Neurol. Sci.* **118:** 188–193, 1993.

MCDONALD W.J., MILLER D.H., BARNES D.: The pathological evolution of multiple sclerosis. *Neuropathol. Appl. Neurol.* **18:** 319–334, 1992.

NAMER I.J., STEIBEL J., POULET P., ARMSPACH J.P., MAUSS Y., CHAMBRON J.: In vivo dynamic MR imaging of MBP-induced acute experimental allergic encephalomyelitis in Lewis rat. *Magnetic Resonance in Medicine* **24:** 325–334, 1992.

NAMER I.J., STEIBEL J., POULET P., ARMSPACH J.P., MOHR M., MAUSS Y., CHAMBRON J.: Blood-brain barrier breakdown in MBP-specific T cell induced experimental allergic encephalomyelitis. A quantitative in vivo MRI study. *Brain* **116:** 147–159, 1993.

NICHOLSON C.: Brain cell microenvironment as a communication channel. In: *The Neuroscience Fourth Study Progress.* F.O. SCHMIDT, F.G. WORDEN (eds), MIT Press, Cambridge, MA, 1979, pp. 457–476.

NICHOLSON C.: Measurement of extracellular space. In: *Practical Electrophysiological Methods: A Guide for in vitro Studies in Vertebrate Neurobiology.* H. KETTENMANN, R. GRANTYN (eds), John Wiley, New York, 1992, pp. 367–372.

NICHOLSON C., PHILLIPS J.M.: Ion diffusion modified by tortuosity and volume fraction in the extracellular microenvironment of the rat cerebellum. *J. Physiol. Lond.* **321:** 225–257, 1981.

NICHOLSON C., RICE M.E.: Diffusion of ions and transmitters in the brain cell microenvironment. In: *Volume Transmission in the Brain, Novel Mechanisms for Neural Transmission.* K. FUXE, L.F. AGNATI (eds), Raven Press, New York, 1991, pp. 279–294.

PENDER M.P., NGUYEN K.B., WILLENBORG D.O.: Demyelination and early remyelination in experimental allergic encephalomyelitis passively transferred with myelin basic protein-sensitized lymphocytes in Lewis rat. *J. Neuroimmunol.* **25:** 125–142, 1989.

RAINE C.S.: Biology of disease. Analysis of autoimmune demyelination: its impact upon multiple sclerosis. *Lab. Invest.* **50:** 608–635, 1984.

SEELDRAYERS P., SYHA J., MORVESSEY S., STODAL H., VASS K., JUNG S., GNEITING T., LASSMANN H., HAASE A., HARTUNG H.P., TOYKA K.: Magnetic resonance imaging investigation of blood brain barrier damage in adoptive transfer experimental autoimmune encephalomyelitis. *J. Neuroimmunol.* **46:** 199–206, 1993.

SIMMONS R.D., BERNARD C.C.A., NG K.T., CARNEGIE P.R.: Hind-limb motor ability in Lewis rats during the onset and recovery phases of experimental autoimmune encephalomyelitis. *Brain Res.* **215:** 103–114, 1981.

SIMMONS R.D., BERNARD C.C.A., SINGER G., CARNEGIE P.R.: Experimental autoimmune encephalomyelitis. An anatomically-based explanation of clinical progression in rodents. *J. Neuroimmunol.* **3:** 307–318, 1982.

SMITH M.E., SOMERA F.P., ENG L.F.: Immunocytochemical staining for glial fibrillary acidic protein and the metabolism of cytoskeletal proteins in experimental allergic encephalomyelitis. *Brain Res.* **264:** 241–253, 1983.

SMITH M.E., SOMERA F.P., SWANSON K., ENG L.F.: Glial fibrillary acidic protein in acute and chronic relapsing experimental allergic encephalomyelitis (EAE). In: *Experimental Allergic Encephalomyelitis. A Useful Model for Multiple Sclerosis.* E.C. ALVORD, M.W. KIES, A.J. SUCKLING (eds), Alan R. Liss, New York, 1984, pp. 139–144.

SVOBODA J., SYKOVÁ E.: Extracellular space volume changes in the rat spinal cord produced by nerve stimulation and peripheral injury. *Brain Res.* **560:** 216–224, 1991.

SYKOVÁ E.: Activity-related ionic and volume changes in neural microenvironment. In: *Volume Transmission in the Brain: Novel Mechanisms for Neural Transmission.* K. FUXE, L.F. AGNATI (eds), Raven Press, New York, 1991, pp. 217–336.

SYKOVÁ E.: Ionic and volume changes in the microenvironment of nerve and receptor cells. In: *Progress in Sensory Physiology.* D. OTTOSON (ed.), Springer, Heidelberg, 1992, pp. 1–167.

SYKOVÁ E., SVOBODA J., POLÁK J., CHVÁTAL A.: Extracellular volume fraction and diffusion characteristics during progressive ischemia and terminal anoxia in the spinal cord of the rat. *J. Cerebr. Blood Flow Metab.* **14:** 301–311, 1994.

VASS K., LASSMANN H., WEKERLE H., WISNIEWSKI H.M.: The distribution of Ia antigen in the lesions of rat acute experimental allergic encephalomyelitis. *Acta Neuropathol.* **70:** 149–160, 1986.

TABIRA T.: Autoimmune demyelination in the central nervous system. *Ann. N.Y. Acad. Sci.* **540:** 187–201, 1988.

WEKERLE H., LININGTON C., LASSMANN H., MEYERMANN R.: Cellular immune reactivity within the CNS. *Trends Neurosci.* **9:** 271–277, 1986.

YU A.C., HERTZ L., NORENBERG M.D., SYKOVÁ E., WAXMAN S. (eds) *Neuronal-Astrocytic Interactions. Implications for Normal and Pathological CNS Function. Progr. Brain Res. Vol. 94*, Elsevier, Amsterdam, 1992.

Reprint Requests
E. Syková, M.D., D.Sc., Institute of Experimental Medicine, Academy of Sciences of the Czech Republic, Department of Cellular Neurophysiology, Vídeňská 1083, 142 20 Prague 4, Czech Republic.